Results in Physics 7 (2017) 3181–3189

Contents lists available at ScienceDirect

Results in Physics

journal homepage: www.journals.elsevier.com/results-in-physics

Stabilized approximation of steady flow of third grade fluid in presence of partial slip

Amer Rasheed [a,*], Azka Kausar [b], Abdul Wahab [c], Tanvir Akbar [d]

[a] Department of Mathematics, School of Science and Engineering, Lahore University of Management Sciences, Opposite Sector U, DHA, Lahore Cantt. 54792, Pakistan
[b] Department of Mathematics, COMSATS Institute of Information Technology, G. T. Road, 47040 Wah Cantt., Pakistan
[c] Bio-imaging and Signal Processing Laboratory, Department of Bio and Brain Engineering, Korea Advanced Institute of Science and Technology, 291, Daehak-ro, Yuseong-gu, 305-701 Daejeon, South Korea
[d] Department of Mathematics, COMSATS Institute of Information Technology, Park Road, 44000 Islamabad, Pakistan

ARTICLE INFO

Article history:
Received 2 July 2017
Accepted 4 August 2017
Available online 13 August 2017

2010 MSC:
76D15
35C15
76A05

Keywords:
Third grade fluid
Partial slip
Streamline-upwind-Petrov-Galerkin
Finite element method

ABSTRACT

This article presents a stable numerical solution to the steady flow of thermodynamic compatible third grade fluid past a porous plate. Problem formulation is completed through partial slip condition. The inability of classical Lagrange-Galerkin methods to provide a stable approximate solution to the envisaged flow problem is demystified. To prevail over the instability issues, a *streamline-upwind-Petrov-Galerkin* method is invoked. The results thus substantiate an apposite agreement with theory. The stability of the approximate solution is testified and appropriate conclusions on flow profile are delineated.

Introduction

It has been generally accepted now that the Newtonian fluids through linear relationship between the stress and rate of strain do not describe several phenomena observed for fluids in industry and other engineering applications. Specifically the viscoelastic flows arise in polymer processing, coating, ink-jet printing, microfluidics, hemodynamics, geological flows in the earth mantle and several others. Modeling and analysis of viscoelastic flows is very important for understanding and predicting the behaviour of processes and thus for designing optimal flow configurations and for operating conditions. Several constitutive equations for viscoelastic fluids have been developed in view of their diverse characteristics (see [1–10] for some recent studies and many related references therein).

The differential type viscoelastic fluids is one of the categories of non-Newtonian fluids. Second grade fluid is simplest subclass of differential type liquids. This type of fluids are able to predict the normal stress effects. However important features of several fluids in terms of shear thinning and shear thickening cannot be predicted be the constitutive equations of second grade fluids. The third grade fluids can capture shear thinning and shear thickening effects even in the steady flow situations. No doubt extra rheological parameters in the constitutive equation of third grade fluid lead to more complex differential system when compared with the second grade fluid. Also the differential system for unidirectional flow of second grade fluid is linear whereas it is nonlinear for third grade fluid. Further the steady unidirectional flow of second grade fluid over rigid surface does not take into account the viscoelastic effects whereas third grade fluid can capture these features easily even in such flow configurations.

The curiosity to understand flows of viscoelastic fluids often triggers challenging and elusive mathematical problems rarely having *exact solutions*. The governing equations related to these flows, like most of the other dynamical systems, are partial differential equations that are strongly non-linear and hard-won to solve. An added difficulty for non-Newtonian, and particularly graded fluids, is the discrepancy between the order of the governing equations

* Corresponding author.
E-mail addresses: amer.rasheed@lums.edu.pk (A. Rasheed), azkakausar@ymail.com (A. Kausar), wahab@kaist.ac.kr (A. Wahab), tanvir.akbar@comsats.edu.pk (T. Akbar).

http://dx.doi.org/10.1016/j.rinp.2017.08.007
2211-3797/

and the number of boundary conditions at hand (*i.e.* fewer conditions than the order). Thus, one requires an over-determined information in order to obtain a unique solution consistent with the corresponding Newtonian flow [11]. Therefore, these flow problems more often do not possess a physically admissible unique closed form analytic solution or even if there exists one, it is really intricate to find and further more daunting to use in practice. Consequently, the approximate and asymptotic solution techniques are in order.

Whenever the rheological parameters are *favorable* and the constitutive equations are weakly non-linear, asymptotic techniques usually lead to convergent series solutions valid over a range of parameters. But for strongly nonlinear problems and for large values of certain characteristic parameters such as *Reynolds*, *Péclet* or *Weissenberg* numbers, these methods fail to produce convergent solutions, leaving only the choice of numerical techniques, see, for example, [12]. However, the *Péclet* and *Reynolds* numbers govern the global stability of the numerical solutions and for convection dominated problems, wherein these parameters have very large values, it is well established that most of the numerical techniques yield unstable solution [13–15]. Nevertheless, numerical strategies have been developed over the recent past in order to overcome the instability of the approximate solutions emerging from strong non-linearity, convection dominance or parabolic-hyperbolic nature of the governing equations. Special attention has been paid to a variety of *upwind Galerkin* and *Petrov-Galerkin* techniques, refer to [14–18] and references contained therein.

The most celebrated stabilized finite element method for convection dominated problems is the *streamline-upwind-Petrov-Galerkin* method, wherein the weight functions are modified by adding a penalty term acting only in the flow direction. The diffusion induced by penalizing the weight functions using streamline upwind effects render a stabilized solution whereas consistent Petrov-Galerkin formulation imparts high order accuracy in the approximation.

The principle concern of this study is the numerical exploration of a graded flow problem. Precisely, flow of a steady incompressible Rivlin-Ericksen fluid of grade three over a horizontal plate with suction or injection subject to a *slip condition* is considered and the approximate fluid velocity field, based on a *streamline-upwind-Petrov-Galerkin* finite element method, is presented. The aim of the present work is two fold:

1. To highlight the convection dominated nature of the aforementioned flow problem and thereby unveiling the inability of standard Galerkin approximation proposed recently in [19].
2. To provide a stabilized formulation to the flow problem thereby providing a stable approximation to the fluid velocity.

In this work, a slip condition is imposed on the fluid velocity at the porous plate. It is frequent to validly presume that the particles adjacent to the boundaries take on the velocity of the boundaries, termed as *no-slip*, that is indeed true for several flows. However, there are situations when these particles move along the boundaries with a finite tangential velocity, different from that of the boundaries rendering a *slip* effect that is strongly dependent on the stress. The references can be made, for example, to the capillary flow of highly entangled polyethylene [20], boundary flow of coating lubricants [21], and flow of pastes of soft particles [22]. Moreover, the *spurt* and *sharkskin* effects in fluids are certainly correlated with the slip effect. We can refer to [10] and references therein for a brief account on slip effect and the historical developments.

The rest of this contribution is arranged in the following manner. The non-dimensional problem formulation is presented in Section "Problem formulation". A naive numerical scheme using classical Lagrange-Galerkin finite element method is provided in Section "Standard Galerkin formulation". A few numerical results are presented to highlight the convection dominated nature of the problem (see Section "Numerical simulations and discussion"). After a brief introduction to convection dominated problems, a stabilized formulation to the flow problem using streamline-upwind-Petrov-Galerkin (SUPG) approach is provided in Section "Streamline-upwind-Petrov-Galerkin formulation". Finally, the findings of the investigation are summarized in Section "Concluding remarks".

Problem formulation

Here we are interested to examine the flow of non-Newtonian fluid past a porous plate at $y=0$. The *x-axis* is taken along the plate while *y-axis* is normal to $x-axis$. The third grade fluid model is considered. The plate is subjected to both effects of uniform suction and injection (or blowing) velocity V_0. Here V_0 corresponds to suction case while $V_0<0$ indicates the blowing phenomenon. The equations relative to flow of an incompressible fluid are

$$\nabla\cdot\mathbf{U}=0, \tag{1}$$

$$\rho\left(\frac{\partial}{\partial t}+\mathbf{U}\cdot\nabla\right)\mathbf{U}=\nabla\cdot\mathbb{T}, \tag{2}$$

where body forces are neglected, t is time and the velocity U in present steady flow consideration is

$$\mathbf{U}=(u(y),-V_0,0), \tag{3}$$

in which u is velocity parallel to the *x-axis*, ρ is the density and constitutive relationship for Cauchy stress tensor $(\mathbb{T})$ in thermodynamic compatible third grade fluid is given by

$$\mathbb{T}=-p\mathbb{I}+\left(\mu+\beta\ \mathrm{tr}\mathbb{A}_1^2\right)\mathbb{A}_1+\alpha_1\mathbb{A}_2+\alpha_2\mathbb{A}_1^2. \tag{4}$$

In above expression p is the fluid pressure, μ the dynamic viscosity, α_1 the viscoelasticity, α_2 the cross viscosity, $\mathbb{I}$ the identity tensor, β the third grade material parameter, tr the trace and the first two Rivlin-Erickson tensors $\mathbb{A}_i$ $(i=1,2)$ satisfy

$$\mathbb{A}_1=\nabla\mathbf{U}+(\nabla\mathbf{U})^{\dagger}, \tag{5}$$

$$\mathbb{A}_2=(\mathbf{U}\cdot\nabla)\mathbb{A}_1+\mathbb{A}_1\nabla\mathbf{U}+(\nabla\mathbf{U})^{\dagger}\mathbb{A}_1, \tag{6}$$

where $\dagger$ signifies the matrix transpose. Now incompressibility condition (1) is identically satisfied and Eqs. (2)–(6) yield

$$\rho v_0\frac{du}{dy}+\mu\frac{d^2u}{dy^2}-\alpha_1 v_0\frac{d^3u}{dy^3}+6\beta_3\left(\frac{du}{dy}\right)^2\frac{d^2u}{dy^2}=0. \tag{7}$$

The partial slip condition in terms of tangential stress becomes

$$u(0)=\frac{\kappa}{\mu}\mathbb{T}_{xy}\bigg|_{y=0}=\frac{\kappa}{\mu}\left[\mu\frac{du}{dy}-\alpha_1 v_0\frac{d^2u}{dy^2}+2\beta_3\left(\frac{du}{dy}\right)^3\right]_{y=0}, \tag{8}$$

where κ is the slip parameter and

$$\lim_{y\to\infty}u(y)=u_\infty. \tag{9}$$

Augmentation process leads to the following definitions

$$\lim_{y\to\infty}\frac{du}{dy}=0\quad\text{and}\quad\lim_{y\to\infty}\frac{d^2u}{dy^2}=0. \tag{10}$$

It is worthmentioning to note that in present case of third grade fluid the condition (8) is nonlinear whereas in second grade fluid it is linear. Even such condition is linear in corresponding flow of third grade fluid when no-slip condition holds.

The resulting boundary value problem can be non-dimensionalized using the following dimensionless quantities,

$$\hat{y} := \frac{\rho u_\infty}{\mu} y, \quad \hat{u} := \frac{u}{u_\infty}, \quad \widehat{v_0} := \frac{v_0}{u_\infty}, \quad \widehat{\alpha_1} := \frac{\rho u_\infty^2}{\mu^2}\alpha_1,$$
$$\widehat{\beta_3} := \frac{\rho^2 u_\infty^4}{\mu^3}\beta_3, \quad \hat{\gamma} := \frac{\rho u_\infty}{\mu}\kappa. \tag{11}$$

By virtue of (11) after dropping the hats for brevity one can write

$$\begin{cases} v_0 \frac{du}{dy} + \frac{d^2u}{dy^2} - \alpha_1 v_0 \frac{d^3u}{dy^3} + 6\beta_3 \left(\frac{du}{dy}\right)^2 \frac{d^2u}{dy^2} = 0, \quad y \in (0,\infty), \\ u(0) = \gamma\left[\frac{du}{dy} - \alpha_1 v_0 \frac{d^2u}{dy^2} + 2\beta_3\left(\frac{du}{dy}\right)^3\right]_{y=0}, \\ \lim_{y\to\infty} u(y) = 1, \quad \lim_{y\to\infty}\frac{du}{dy} = 0, \quad \lim_{y\to\infty}\frac{d^2u}{dy^2} = 0. \end{cases} \tag{12}$$

On integrating first equation in (12) over $(y, +\infty)$ and using conditions at infinity, we obtain

$$v_0 u + \frac{du}{dy} - \alpha_1 v_0 \frac{d^2u}{dy^2} + 2\beta_3\left(\frac{du}{dy}\right)^3 = v_0 \tag{13}$$

The above equation together with the partial slip condition yields

$$u(0) = \frac{\gamma v_0}{1+\gamma v_0}. \tag{14}$$

Hence the velocity field u finally satisfies the following boundary value problem:

$$\begin{cases} -\alpha_1 v_0 \frac{d^2u}{dy^2} + \frac{du}{dy} + v_0 u + 2\beta_3\left(\frac{du}{dy}\right)^3 = v_0, \quad y \in (0,\infty), \\ u(0) = \frac{\gamma v_0}{1+\gamma v_0} \quad \text{and} \quad \lim_{y\to\infty} u(y) = 1. \end{cases} \tag{15}$$

Standard Galerkin formulation

This section is in order to demystify the inability of the standard Galerkin finite element method for providing a stable approximation to the velocity field u satisfying (15). We will proceed here with a naive Galerkin discretization to fix the ideas related to approximation and interpolation spaces. This will also serve as a building block for the endeavor to obtain a stable finite element solution using an SUPG-method discussed in the next section.

Since the boundary value problem (15) is defined on a physical domain $(0,+\infty)$, one must truncate the domain to a synthetic artificial bounded domain in order to deploy a finite element method. However, to render a well-posed boundary value problem in the interior domain whose solution is compatible with the original one over the physical domain, an artificial boundary condition over the boundaries emerging from the domain truncation is indispensable. Refer to [23,24] and references therein for instance for a detailed discussion on imposing valid artificial boundary conditions. However, since the velocity satisfying (15) approaches to a uniform main stream velocity which is equal to 1, we have $u(y) \simeq 1$ at large values of y by virtue of the far field boundary condition $\lim_{y\to\infty} u(y) = 1$. Therefore in the present study it is sufficient to truncate the physical domain to a bounded domain $(0, y_{\max})$ with $y_{\max}$ being very large to mimic $+\infty$ so that $u(y_{\max}) \simeq 1$. Precisely we consider the following boundary value problem to model the velocity profile henceforth:

$$\begin{cases} -\alpha_1 v_0 \frac{d^2u}{dy^2} + \frac{du}{dy} + v_0 u + 2\beta_3\left(\frac{du}{dy}\right)^3 = v_0, \quad y \in (0,y_{\max}), \\ u(0) = \frac{\gamma v_0}{1+\gamma v_0} \quad \text{and} \quad u(y_{\max}) = 1. \end{cases} \tag{16}$$

By virtue of the transformation

$$w(y) = u(y) - u_H(y) \quad \text{with} \quad u_H(y) = u(0) + \frac{y}{y_{\max}}(1-u(0)), \tag{17}$$

the boundary value problem (16) yields

$$\begin{cases} -\alpha_1 v_0 \frac{d^2w}{dy^2} + \beta\frac{dw}{dy} + v_0 w(y) + \mathcal{N}(w) = f(y), \\ w(0) = 0 = w(y_{\max}), \end{cases} \tag{18}$$

with

$$\mathcal{N}(w) = 2\beta\left[\left(\frac{dw}{dy}\right)^3 + 3\delta_0\left(\frac{dw}{dy}\right)^2\right] \quad \text{and} \quad f(y) = -(v_0 u_H + v_1), \tag{19}$$

where

$$\delta_0 = \frac{1}{y_{\max}}(1-u(0)), \quad \beta = 1 + 6\beta_3\delta_0^2 \quad \text{and} \quad v_1 = 2\beta\delta_0^3 + \delta_0 - v_0. \tag{20}$$

In the rest of the section, a numerical exposition of the boundary value problem (18) is provided which together with transformation (17) helps us to infer on the stability of the approximate solution to the flow problem (16).

Variational formulation

This section is dedicated to present a weak form of the problem (18) and to collect a few notions and notations indispensable for spatial discretization of the flow problem. Henceforth, the space $L^2(\Omega)$ equipped with the inner product and norm respectively defined as

$$(\phi,\psi)_{L^2(\Omega)} = (\phi,\psi) = \int_\Omega \phi\psi dy \quad \text{and} \quad \|\phi\|_{L^2(\Omega)} = \|\phi\| = \left(\int_\Omega |\phi|^2 dy\right)^{1/2} \tag{21}$$

represents the space of square integrable functions over the domain $\Omega = (0, y_{\max})$. Further, $H^1(\Omega)$ denotes the usual Sobolev space and $H_0^1(\Omega)$ denotes the closure of $\mathscr{C}_0^\infty(\overline{\Omega})$ in $H^1(\Omega)$ where $\mathscr{C}_0^\infty(\overline{\Omega})$ represents the space of infinitely continuous functions with compact support in Ω; see for instance [25]. Recall that $H^1(\Omega)$ and $H_0^1(\Omega)$ are equipped with following inner products and norms,

$$(\phi,\psi)_{H^1} := (\phi,\psi)_1 = (\phi,\psi) + \left(\frac{d\phi}{dy},\frac{d\psi}{dy}\right) \quad \text{and}$$
$$(\phi,\psi)_{H_0^1} := (\phi,\psi)_0 = \left(\frac{d\phi}{dy},\frac{d\psi}{dy}\right), \tag{22}$$

$$\|\phi\|_{H^1} := \|\phi\|_1 = \left(\|\phi\|^2 + \left\|\frac{d\phi}{dy}\right\|^2\right)^{1/2} \quad \text{and}$$
$$\|\phi\|_{H_0^1} := \|\phi\|_0 := |\phi|_1 = \left\|\frac{d\phi}{dy}\right\|, \tag{23}$$

where $|\cdot|_1$ represents a semi-norm in $H^1(\Omega)$. Equipped with the aforementioned notions and notations, we are now in position to introduce the following weak form of the flow problem (18).

Weak Form. Find $w \in H_0^1(\Omega)$ such that

$$b(w,\phi) + (\mathcal{N}(w),\phi) = l(\phi) \quad \text{for all} \quad \phi \in H_0^1(\Omega), \tag{24}$$

where $l : H_0^1(\Omega) \to \mathbb{R}$ and $b : H_0^1(\Omega) \times H_0^1(\Omega) \to \mathbb{R}$ are respectively defined by

$$l(\phi) := (f,\phi) \quad \text{and} \quad b(\phi,\psi) :$$
$$= \alpha_1 v_0\left(\frac{d\phi}{dy},\frac{d\psi}{dy}\right) - \beta\left(\phi,\frac{d\psi}{dy}\right) + v_0(\phi,\psi). \quad \square \tag{25}$$

Lagrange-Galerkin finite element approximations

Let $0 = y_1 < y_2 < \cdots < y_n < y_{n+1} = y_{\max}$. Define the partition of the domain Ω into n subdomains $\Omega_i = (y_i, y_{i+1})$ for $i = 1, 2, \ldots, n$ such that

$$\overline{\Omega} = \bigcup_{i=1}^{n} \overline{\Omega}_i \quad \text{and} \quad \Omega_i \bigcap \Omega_j = \varnothing, \quad \forall i \neq j.$$

Let each element $\overline{\Omega}_i$ has n_e local nodes $y_i^1 < y_i^2 < \cdots < y_i^{n_e}$; such that $y_i^1 = y_i$ and $y_i^{n_e} = y_{i+1}$. Further assume that h is the uniform length of elements Ω_i, that is,

$$h := \frac{y_{\max}}{n} := y_{i+1} - y_i.$$

Define a sequence of finite dimensional approximation subspaces $\left\{ \mathscr{V}_0^h(\Omega) \right\}_{h>0}$ of $H_0^1(\Omega)$ by

$$\mathscr{V}_0^h(\Omega) := \left\{ \phi \in H_0^1(\Omega) \;\middle|\; \phi_{|_{\Omega_i}} \in \mathscr{P}_k(\Omega_i),\ \forall i = 1, 2, \ldots, n \right\}, \tag{26}$$

where $\mathscr{P}_k(\Omega_i), k \geqslant 1$ is a finite element interpolation space of polynomials with degree at most k over each element Ω_i. With an aim to approximate the unknown function $w \in H_0^1(\Omega)$ with $w_h \in \mathscr{V}_0^h(\Omega)$, we interpolate w over each element Ω_i. The approximate solution $w_h^i \in \mathscr{V}_0^h(\Omega)$ over Ω_i can be obtained as

$$w_h^i(y) = \sum_{j=1}^{n_e} w_j^i \psi_j^i(y), \quad y \in \overline{\Omega}_i = [y_i, y_{i+1}], \tag{27}$$

where w_j^i is the unknown nodal value of the function w_h^i at the local node y_i^j, where $j = 1, 2, \cdots, n_e$. Here ψ_j^i are the interpolation polynomial basis elements of degree k associated with local nodes y_i^j over the element Ω_i defined by the relation $\psi_j^i(y_i^m) = \delta_{jm}$, where δ_{jm} denotes the Kronecker's delta. In the same spirit, the discrete weak formulation of the flow problem (18) is given by

Discrete Weak Form. Find $w_h^i \in \mathscr{V}_0^h(\Omega)$ for $i = 1, 2, \ldots, n$, such that

$$b(w_h^i, v_h) + \left(\mathscr{N}(w_h^i), v_h\right) = l(v_h) \quad \text{for all} \quad v_h \in \mathscr{V}_0^h(\Omega) \quad \text{and} \quad y \in \overline{\Omega}_i. \quad \square \tag{28}$$

Substituting ansatz (27) in the discrete weak form (28) and choosing v_h as the basis elements ψ_j^i, we arrive at the non-linear system of equations

$$\mathbb{A}_h^i \mathbf{W}^i + \mathbf{N}^i(\mathbf{W}^i, \Psi^i) = \mathbf{F}^i(\Psi^i), \tag{29}$$

where for $p, q \in \{1, 2, \ldots, n_e\}$,

$$\begin{cases} \left(\mathbf{W}^i\right)_p := w_p^i, \quad \left(\Psi^i\right)_p := \psi_p^i, \quad \left(\mathbf{F}^i\right)_p := \left(f, \psi_p^i\right), \quad \left(\mathbf{N}^i\right)_p := \left(\mathscr{N}, \psi_p^i\right), \\ \left(\mathbb{A}_1^i\right)_{qp} := \left(\frac{d\psi_p^i}{dy}, \frac{d\psi_q^i}{dy}\right), \quad \left(\mathbb{A}_2^i\right)_{qp} := \left(\psi_p^i, \frac{d\psi_q^i}{dy}\right), \quad \left(\mathbb{A}_3^i\right)_{qp} := \left(\psi_p^i, \psi_q^i\right), \\ \mathbb{A}_h^i := \alpha_1 v_0 \mathbb{A}_1^i - \beta \mathbb{A}_2^i + v_0 \mathbb{A}_3^i. \end{cases} \tag{30}$$

The non-linear system of Eq. (29) can be written in terms of a non-linear function $\mathbf{G} : \left(\mathscr{V}_0^h(\Omega)\right)^{N_h} \to \mathbb{R}^{N_h}$ as

$$\mathbf{G}(\mathbf{W}) := \mathbb{A}_h \mathbf{W} + \mathbf{N}(\mathbf{W}) - \mathbf{F}(\Psi) = \mathbf{0}, \tag{31}$$

where $N_h = \dim\left(\mathscr{V}_0^h\right)$. In order to find $\mathbf{W}$ satisfying (31), one requires the use of an iterative procedure. In the following, a Newton iteration method is invoked to solve (31). The following algorithm explains the basic structure of the numerical scheme which is then implemented in MatLab to carryout the simulations.

Implementation scheme

i Initialize the input parameters involved in the matrix equations, such as α_1, β, and v_0.
ii Create a mesh with n elements $\Omega_i,\ i = 1, 2, \ldots, n$ having $n+1$ nodes.
iii Allocate memory for the global matrix $\mathbb{A}_h$, Jacobian matrix $\mathscr{J}$ of non-linear function $\mathbf{G}$ of order $(N_h+1) \times (N_h+1)$, vectors $\mathbf{N}$ and $\mathbf{F}$ of order $(N_h+1) \times 1$ and initialize all matrix entries to zero.
iv Initialize and start **While** loop for Newton iterations.
  a. **For** $i = 1, 2, 3, \ldots, n$, **do** Compute the element stiffness matrix $\mathbb{A}_h^i$, non-linear vector $\mathbf{N}^i$ and right hand side vector $\mathbf{F}^i$.
  b. Add element matrices into the corresponding global matrices at respective positions.
  c. Find the Jacobian matrix $\mathscr{J}$.
  d. Apply the Newton's iteration to update the solutions.
  Terminate the **While** loop.
v Apply boundary conditions and plot the solutions.

Numerical simulations and discussion

In this section, we demystify the numerical instability of Galerkin approach detailed in the previous subsection for the flow problem (15). The numerical tests are performed with $\mathscr{P}_2$ Lagrange interpolation functions with $y_{\max} = 10$ and the following initial guess for the Newton iteration method

$$\widetilde{u}(y) = 1 - ((1 - u(0))e^{-\alpha_1 v_0 y}. \tag{32}$$

In Figs. 1–2, a comparison of the fabricated exact solution u is made with the approximate solution u_h for different choices of viscoelasticity modulus α_1 and cross flow velocity v_0. Two different behaviors of the numerical solutions are observed. When α_1 and v_0 have large values, the Galerkin solution is in good agreement with the exact one. However, when $\alpha_1 v_0 \to 0$ the flow problem becomes convection dominated and node to node oscillations appear in the numerical solutions.

Streamline-upwind-Petrov-Galerkin formulation

The appositeness of standard finite element methods, especially Galerkin methods, to evince most elliptic, structural and heat flow problems thereby providing highly accurate approximate solutions to them is well established. This is indeed due to symmetric nature of the associated stiffness matrices. In many engineering applications, for example, in fluid flows or convective heat transfer problems where convection is really dominant, these methods do not work adequately and give spurious oscillations in the approximations. The *Péclet* numbers expressing the inter-relation of convection and diffusion govern the global stability of the numerical solutions. Their high values lead to the generation of interior and boundary layers, indeed, due to the vanishing nature of the highest order derivative with a significant one of first order. Consequently, classical methods produce oscillations around high gradient regions corrupting the approximate solution since these oscillations travel along in the entire domain by the convection as an automotive force. On the other hand, the favoring symmetry of the stiffness matrices is lost, thereby producing only sub-optimal results; refer to [13,14].

Different remedies to numerical instability caused by convection dominance have been proposed. One way to avoid the wiggles in the approximate solutions is to drastically refining the mesh so that convection dissipates on an element level thereby rendering the element *Péclet* numbers very small compared to the global one. However, this is computationally very expensive. In view of

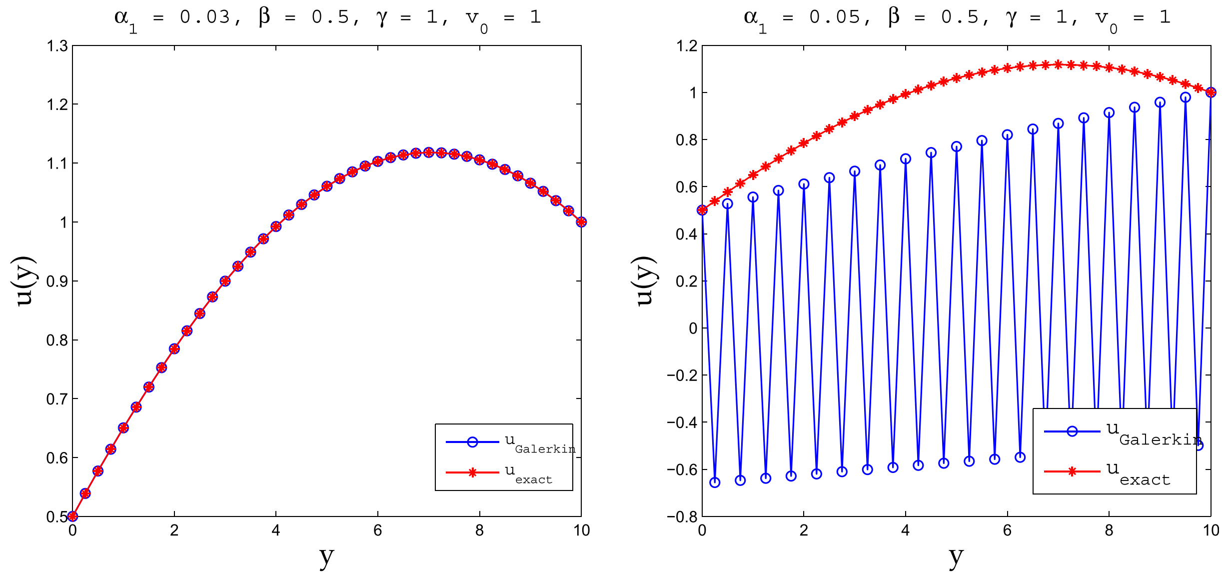

Fig. 1. Comparison of the exact solution with approximate solution using standard Galerkin approach for viscoelasticty modulus $\alpha_1 = 0.03$ (left) and $\alpha_1 = 0.05$ (right).

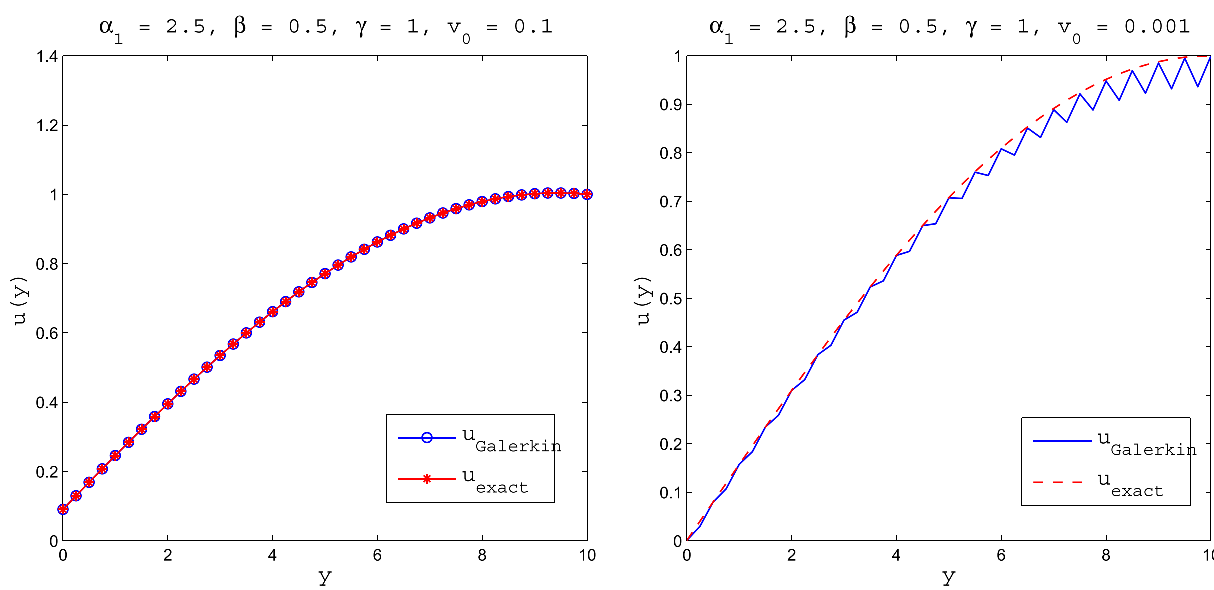

Fig. 2. Comparison of the exact solution with approximate solution using standard Galerkin approach for cross flow velocity $v_0 = 0.1$ (left) and $v_0 = 0.001$ (right).

their analogy with central difference approximations, introducing upwind effects in Galerkin methods is another approach to prevent instability in the approximate solutions to convection dominated problems. Several upwind techniques have been developed and understood, see, for instance, [16,18]. These methods have shown significant improvements over the classical Galerkin methods for the linear homogeneous convective models. Unfortunately, for more general problems or in higher dimensions wherein source term or non-linearity is involved these methods fail to give adequate approximate solutions.

The *streamline-upwind-Petrov-Galerkin (SUPG)* technique of Brooks & Hughes [14] is one of the most powerful and robust upwind techniques which tackles the intrinsic deficiencies of other upwind finite element methods while keeping the stabilization effects intact. This technique is based on the idea that the upwind effect is only required along streamlines. This is in contrast to other upwind techniques wherein Galerkin methods are inconsistently augmented with an artificial diffusion for the purpose and fail to produce satisfactory results due to the *crosswind diffusion*. In SUPG technique, the upwind effects are introduced in consistent Petrov-Galerkin formulations only along the streamlines by perturbing classical weight functions using a discontinuous perturbation acting in the direction of the flow. As a consequence, it provides a stabilized solution with same order of accuracy as offered by standard Galerkin formulations [13–15].

Stabilized formulation

The aim here is to adopt SUPG finite element technique to stabilize the numerical approximation of the fluid velocity. We start by precising that the *Péclet* number associated with flow problem (16) is given by $\mathrm{Pe} := \frac{1}{\alpha_1 v_0}$.We also define the element *Péclet* number by $\mathrm{Pe}^h := \frac{h}{2\alpha_1 v_0}$. The initial step of the SUPG technique is to augment the standard weight functions $v_h \in \mathscr{V}_0^h$ by a perturbation proportional to $\frac{dv_h}{dy}$, that is, the weight functions are taken to be

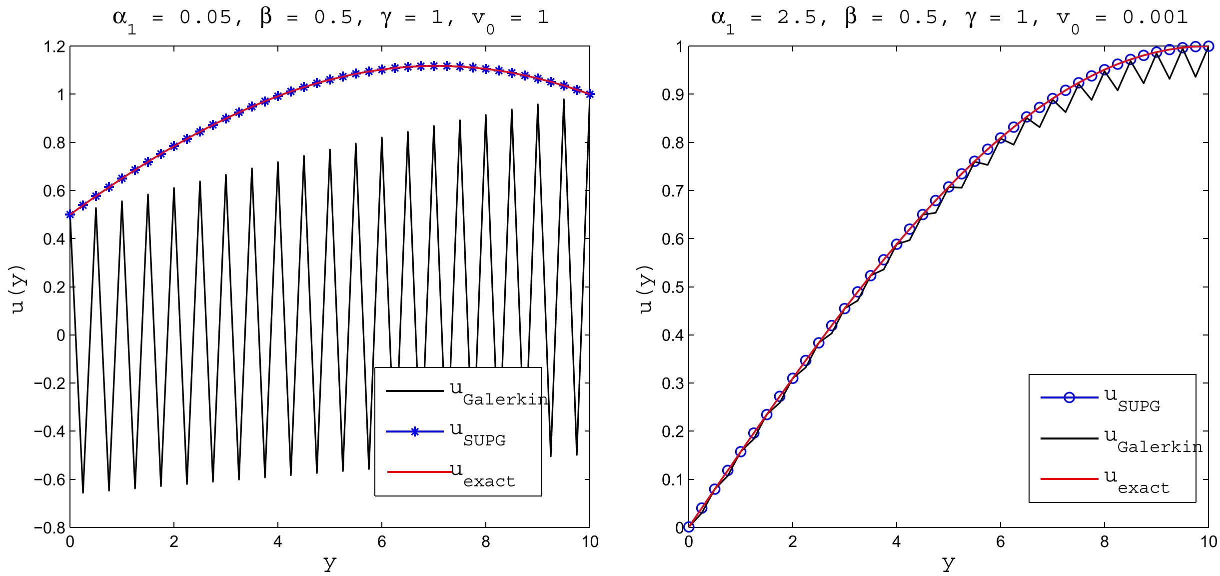

Fig. 3. Comparison of the exact solution with approximate solution using standard Galerkin and SUPG formulations for $(\alpha_1, v_0) = (0.05, 1)$ (left) and $(\alpha_1, v_0) = (2.5, 001)$ (right).

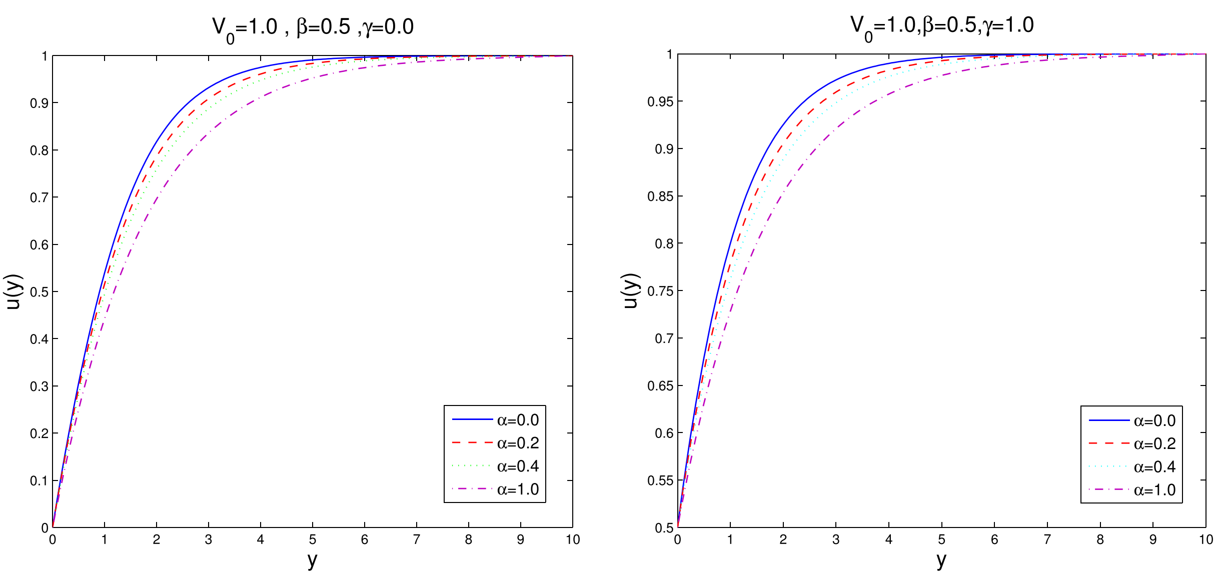

(a) No-slip (b) Partial-slip

Fig. 4. Influence of α_1 on the fluid velocity u.

$$\widetilde{v}_h := v_h + \tau \frac{dv_h}{dy}, \quad \forall v_h \in \mathscr{V}_0^h, \tag{33}$$

where τ, coined as *intrinsic time*, is a stabilization parameter optimally controlling the amount of artificial diffusion needed while retaining high order accuracy. Since, the functions v_h are piecewise polynomials, they are infinitely differentiable inside each element but merely continuous at the nodes. Thus $\widetilde{v}_h$ are jump-discontinuous and consequently their derivatives involve *Dirac-delta* at inter-element boundaries. This forbids the integration over Ω in the modified weighted formalism. However, the ostensible difficulty can be precluded by stabilizing only inside the interior of the elements. This further helps to maintain the global continuity requirements [15].

In the sequel, we coin the following as stabilized weak form of the flow problem (16).

Stabilized Form. Find $w_h \in \mathscr{V}_0^h(\Omega)$ such that

$$b(w_h, v_h) + (\mathscr{N}(w_h), v_h) + \sum_{i=1}^{n} \tau_i \left(\mathscr{R}_h(w_h), \frac{dv_h}{dy} \right)_{\Omega_i} = l(v_h) \quad \text{for all} \quad v_h \in \mathscr{V}_0^h(\Omega), \tag{34}$$

where $\mathscr{R}_h(\phi) := -\alpha_1 v_0 \frac{d^2\phi}{dy^2} + \beta \frac{d\phi}{dy} + v_0\phi + \mathscr{N}(\phi) - f$ is the residual, $(\phi, \psi)_{\Omega_i} := \int_{\Omega_i} \phi\psi dy$ and

$$\tau_i := \frac{h}{2} \vartheta_i^j \left(\mathrm{Pe}^h \right), \quad j = 1, 2, \ldots, n_e. \tag{35}$$

Here $\vartheta_i^j = \vartheta_i^j \left(\mathrm{Pe}^h \right)$ are called the upwind functions. □

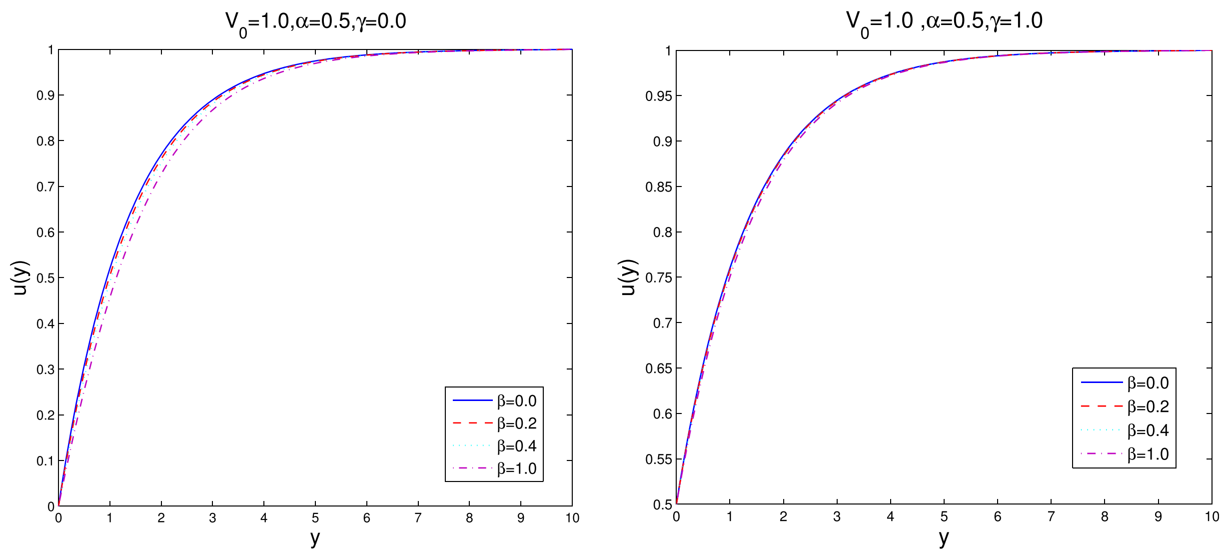

(a) No-slip (b) Partial-slip

Fig. 5. Influence of β on the fluid velocity u.

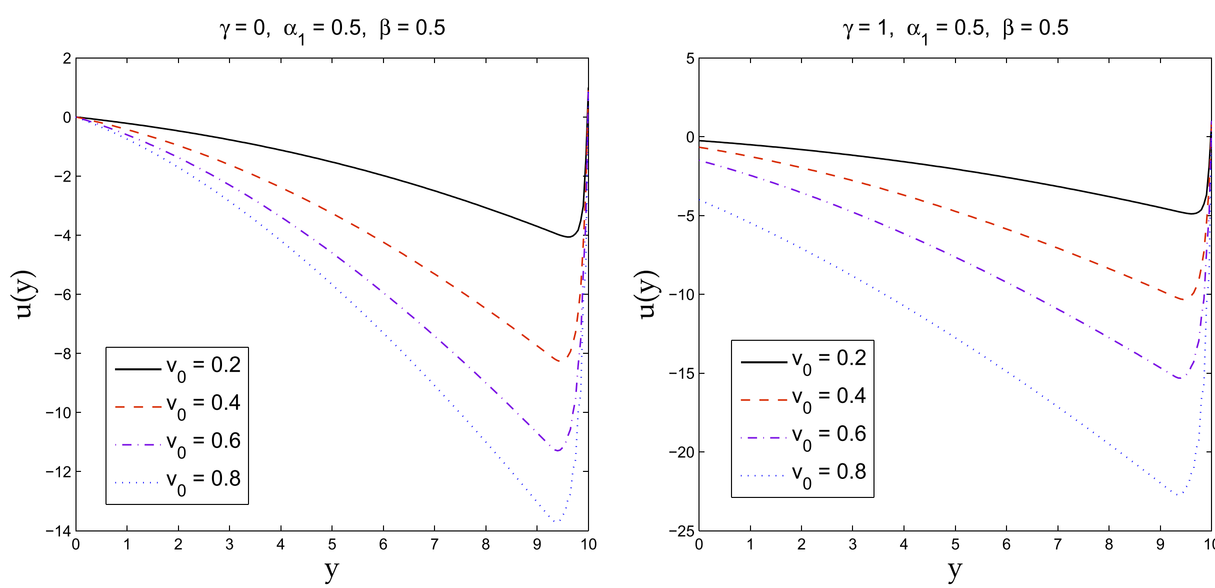

(a) No-slip (b) Partial-slip

Fig. 6. Influence of suction velocity v_0 on the fluid velocity u.

Remark. The upwind functions ϑ_i^j are chosen in such a way that the upwind solution becomes nodally exact. For $\mathscr{P}_1$ and $\mathscr{P}_2$ elements, these functions can be given respectively by; refer to [17]

$$\vartheta_i^j := \left(\coth(\mathrm{Pe}^h) - \frac{1}{\mathrm{Pe}^h}\right), \quad j = 1, 2, \tag{36}$$

and

$$\begin{cases} \vartheta_i^2 := \frac{1}{2}\left(\coth\left(\frac{\mathrm{Pe}^h}{2}\right) - \frac{2}{\mathrm{Pe}^h}\right) \\ \vartheta_i^j := \frac{(3+3\mathrm{Pe}^h)\tanh(\mathrm{Pe}^h) - \left(3\mathrm{Pe}^h + (\mathrm{Pe}^h)^2 \vartheta_i^2\right)}{\left(2-3\vartheta_i^2 \tanh(\mathrm{Pe}^h)\right)(\mathrm{Pe}^h)^2}, \quad j = 1, 3. \end{cases} \tag{37}$$

For a given segment Ω_i and weight functions

$$\widetilde{\psi}_j^i := \psi_j^i + \vartheta_i^j \frac{h}{2}\frac{d\psi_j^i}{dy}, \quad j = 1, 2, \ldots, n_e,$$

Eq. (34) yields

$$b(w_h^i, \psi_j^i) + \left(\mathscr{N}(w_h^i), \psi_j^i\right) + \frac{h}{2}\vartheta_i^j \left(\mathscr{R}_h(w_h^i), \frac{d\psi_j^i}{dy}\right)_{\Omega_i} = l(\psi_j^i) \quad \text{for all} \quad y \in \overline{\Omega}_i, \tag{38}$$

This, together with the ansatz (27), leads to the following system of non-linear equations

$$\widetilde{\mathbb{A}}_h^i \mathbf{W}^i + \widetilde{\mathbb{B}}_h^i \mathbf{W}^i + \widetilde{\mathbf{N}}^i(\mathbf{W}^i, \Psi^i) = \widetilde{\mathbf{F}}^i(\Psi^i), \tag{39}$$

where for $p, q \in \{1, 2, \ldots, n_e\}$,

$$\begin{cases} \left(\widetilde{\mathbb{A}}_h^i\right)_{pq} := \left(\mathbb{A}_h^i\right)_{pq} - \frac{h\vartheta_i^p}{2}\left[\beta\left(\frac{d\psi_q^i}{dy}, \frac{d\psi_p^i}{dy}\right)_{\Omega_i} - v_0\left(\psi_q^i, \frac{d\psi_p^i}{dy}\right)_{\Omega_i}\right], \\ \left(\widetilde{\mathbb{B}}_h^i\right)_{pq} := -\alpha_1 v_0 \frac{h\vartheta_i^p}{2}\left(\frac{d^2\psi_q^i}{dy^2}, \frac{d\psi_p^i}{dy}\right)_{\Omega_i}, \\ \left(\widetilde{\mathbf{N}}^i\right)_p := \left(\mathbf{N}^i\right)_p + \frac{h\vartheta_i^p}{2}\left(\mathcal{N}, \frac{d\psi_p^i}{dy}\right)_{\Omega_i}, \\ \left(\widetilde{\mathbf{F}}^i\right)_p := \left(\mathbf{F}^i\right)_p + \frac{h\vartheta_i^p}{2}\left(f, \frac{d\psi_p^i}{dy}\right)_{\Omega_i}. \end{cases} \quad (40)$$

Stablized numerical illustrations

For further discussion and numerical results in this section, we restrict ourselves only to $\mathscr{P}_2$ interpolation functions. The numerical tests are performed with $y_{\max} = 10$ and the initial guess for the Newton iteration method is taken as

$$\widetilde{u}(y) = 1 - ((1 - u(0))e^{-\alpha_1 v_0 y}. \quad (41)$$

Appositeness of SUPG formulation

As observed in Section "Numerical simulations and discussion", when the flow problem (16) is diffusion dominated, classical Galerkin method provides a numerical solution in good agreement with the exact one. However, when $\alpha_1 v_0 \to 0$, Eq. (16) becomes convection dominated and numerical oscillations appear in the approximate solution as delineated in Figs. 1 and 2. Nevertheless, Fig. 3 substantiates that the solution obtained using stabilized formulation is wiggle-free as well as precise even when the global *Péclet* number is very large.

Characteristic behavior of velocity profile

In Figs. 4–7, the impact of characteristic rheological parameters on the fluid velocity u is evinced. Fig. 4 indicates that the amplitude of velocity field decreases with increasing values of the viscoelasticity modulus α_1, no matter whether a no slip or a partial slip condition is imposed. Similar dependence of u on third grade modulus β can be observed in Fig. 5. On the other hand, velocity u is a decreasing function of the cross flow velocity v_0, refer to Fig. 6. Moreover Fig. 7 also elucidates that u is an increasing function of the boundary slip parameter γ. Further, the boundary layer thickness decreases when we increase any of the parameters α_1, β, v_0 or γ.

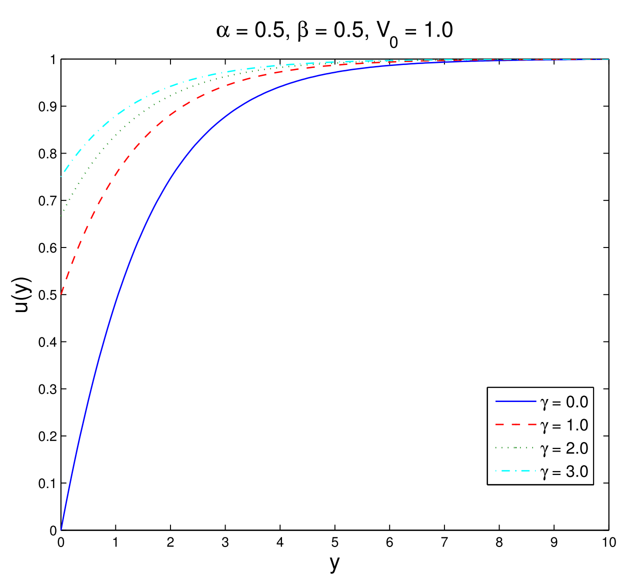

Fig. 7. Influence of the slip parameter γ on the fluid velocity u.

From Figs. 5 and 6, it is apparent that the partial slip condition retards the variations in u with respect to β whereas it enhances the variations in u with respect to v_0 compared to the case of a no-slip condition. However, in Fig. 4, no significant change in the variation of u with respect to α_1 is observed in slip and no-slip situations, apart from altering the initial amplitude of the velocity field.

Concluding remarks

In this work, numerical approximation of the velocity profile to the steady flow of third grade fluid past a porous plate with partial slip condition is made. Due to its convection dominated nature, the classical Galerkin approach is not suitable to resolve the considered flow problem. The application of a streamline-upwind-Pet rov-Galerkin technique is thus motivated and numerical results, appropriately taking care of the underlying convection dominance, are presented. The characteristic behavior of the velocity profile with respect to influential flow parameters is discussed.

Competing interests

All the authors declare that they have no competing interests.

Author's contributions

All the authors have contributed in writing and approved the article.

Acknowledgments

The authors are thankful to all the reviewers for their recommendations to improve the quality of the article.

References

[1] Fetecau C, Imran MA, Axinte E, Fetecau C. On the energetic balance for the flow of an Oldroyd-B fluid induced by a constantly accelerating plate. Zeitschift Fur Angewandte Mathematik Und Physik 2010;61(6):1085–95.
[2] Jun N, Zai-hong S, Tan WC. The viscoelastic effects on thermal convection of an Oldroyd-B fluid in open-top porous media. J Hydrodyn, Ser B 2013;25 (4):639–42.
[3] Jamil M, Fetecau C, Imran M. Unsteady helical flows of Oldroyd-B fluids. Commun Nonlinear Sci Numer Simul 2011;16(3):1378–86.
[4] Hussain M, Hayat T, Asghar S, Fetecau C. Oscillatory flows of second grade fluid in a porous space. Nonlinear Anal-Real World Appl 2010;11(4):2403–14.
[5] Fetecau C, Athar M, Fetecau C. Unsteady flow of a generalized Maxwell fluid with fractional derivative due to a constantly accelerating plate. Comput Math Appl 2009;57(4):596–603.
[6] Hayat T, Khalid Umbreen, Qasim M. Steady flow of a Williamson fluid past a porous plate. Asia-Pacific J Chem Eng 2012;7(2):302–6.
[7] Hayat T, Zaib S, Asghar S, Hendi AA. Exact solutions in generalized Oldroyd-B fluid. Appl Math Mech Engl Ed 2012;33(4):411–26.
[8] Wenchang Tan, Wenxiao Pan, Mingyu Xu. A note on unsteady flows of a viscoelastic fluid with the fractional Maxwell model between two parallel plates. Int J Non Linear Mech 2003;38:645–50.
[9] Xue C, Nie J, Tan WC. An exact solution of start-up flow for the fractional generalized Burgers fluid in a porous half-space. Nonlinear Anal: Theory Methods Appl 2008;69(7):2086–94.
[10] Rashidi MM, Hayat T, Erfani E, Pour SAM, Hendi AA. Simultaneous effects of partial slip and thermal-diffusion and diffusion-thermo on steady MHD convective flow due to a rotating disk. Commun Nonlinear Sci Numer Simul 2011;16(11):4303–17.
[11] Ariel PD. Flow of a third grade fluid through a porous flat channel. Int J Eng Sci 2003;41:1267–85.
[12] Lipscombe TC. Comment on 'Application of the homotopy method for analytical solution of non-Newtonian channel flows'. Phys Scr 2010;81. Article ID. 037001.
[13] Brooks AN, Petrov-Galerkin A. Finite element formulation for convection dominated flows [PhD. Dissertation]. California Institute of Technology; 1981.
[14] Brooks AN, Hughes TJR. Streamline Upwind/Petrov-Galerkin formulations for convection dominated flows with particular emphasis on the incompressible Navier-Stokes equations. Comput Methods Appl Mech Eng 1982;32:199–259.

[15] Fries T-P, Matthies HG. A review of Petrov-Galerkin stabilization approaches and an extension to meshfree methods. Technical Report: Informatikbericht 200401. Institute of Scientific Computing. Technical University Braunschweig.
[16] Christie I, Griffiths DF, Mitchell AR, Zienkiewicz OC. Finite element methods for second order equations with significant first derivatives. Int J Numer Methods Eng 1976;10:1389–96.
[17] Codina R, Oñate E, Cervera M. The intrinsic time for the streamline upwind/Petrov-Galerkin formulation using quadratic elements. Comput Meth Appl Mech Eng 1992;94:239–62.
[18] Heinrich J, Huyakorn PS, Zienkiewicz OC, Mitchell AR. An 'upwind' finite element scheme for two dimensional convective transport equation. Int J Numer Methods Fluids 1977;11:134–43.
[19] Sajid M, Mahmood R, Hayat T. Finite element solution for flow of a third grade fluid past a horizontal porous plate with partial slip. Comput Math Appl 2008;56:1236–44.
[20] Wang S-Q, Drda PA. Stick-slip transition in capillary flow of linear polyethylene: surface conditions. Rheol Acta 1997;36:128–34.
[21] Triantafillopoulos N, Kokko A, Grankvist T. Apparent slip of paper coatings and the influence of coating lubricants. Tappi J 2001;84(7):58.
[22] Meeker SP, Bonnecaze RT, Cloitre M. Slip and flow in pastes of soft particles: direct observation and rheology. J Rheol 2004;48(6):1295–320.
[23] Heywood JG, Rannachar R, Turek S. Artificial boundaries and flux and pressure conditions for the incompressible Navier-Stokes equations. Int J Numer Methods Fluids 1996;22:325–52.
[24] Papanastasiou TC, Malamataris N, Ellwood K. A new outflow boundary condition. Int J Numer Methods Fluids 1992;14:587–608.
[25] Adams RA. Sobolev spaces. New York: Academic Press; 1975.